THE IMPORTANCE OF IMPACTOR COMPOSITION ON THE GEOPHYSICAL CONSEQUENCES OF PLANETARY-SCALE IMPACTS INTO A MARS-LIKE PLANET. M. M. Marinova[1,2], O. Aharonson[3], and E. Asphaug[4], [1]BAER Institute (margarita.m.marinova@gmail.com), [2]Space Sciences Division, NASA Ames Research Center, [3]Division of Geological and Planetary Sciences, California Institute of Technology, [4]Earth and Planetary Sciences Dept., University of California, Santa Cruz.

Introduction: Planetary-scale impacts were ubiquitous in the final stages of planetary accretion, when the last few planetesimals accreted onto the planets. These impacts had a notable effect on the planets, as they contributed significant energy, mass, and angular momentum to these already mostly-formed objects [1].

In the planetary-scale impact regime, the crater cavity is a large fraction of the planetary circumference, and the planet curvature, radial gravity, and large relative size of impactor to target are important, unlike for small, effectively half-space in geometry, impacts.

The impactors in planetary-scale impacts, were likely differentiated, due to the late timing of the events [2] and their size being similar to, or larger than, differentiated asteroids such as Ceres (940 km diameter [3]) and Vesta (520 km diameter [4,5]). However, the exact internal structure and composition of the impactors is uncertain, and could have varied appreciably.

Here we explore the geophysical consequences of a range of impactor compositions, particularly differentiated impactors (olivine and iron), and single-composition olivine (density of 3,500 kg/m^3), undifferentiated (4,570 kg/m^3), and iron (7,800 kg/m^3) impactors, and how these compare to the previously-studied basalt impactors (2,700 kg/m^3 [1]). These end-member compositions encompass the range of non-icy impactor densities and internal structures that could have comprised the planetary-scale impactors. For a given impact energy and velocity, variations in the impactor composition, and thus density, correspond to difference in impactor size, and affect the relative buoyancy of the impactor with respect to the planetary mantle. In the case of differentiated impactors, the significant density difference between the impactor mantle and core results in a complicated interaction with the planet. The undifferentiated impactor is simulated by a single material with a density equivalent to the proportional mixture of materials.

Studying this new broad range of impactor types allows a comprehensive characterization of the geophysical consequences of planetary-scale impacts, and their expected morphological expression on the planetary surface. These results offer better interpretation of the formation mechanism of large impact structures observed on other planets.

Modeling: We use the fully three-dimensional smoothed particle hydrodynamics (SPH) model originally developed by Benz [6] to simulate the impacts. SPH is a Lagrangian model, where continuous matter is represented by a collection of smoothed particles or kernel functions (fig. 1). This SPH model has been previously used to simulate planetary-scale impacts [1], as well as the more energetic giant impacts [e.g., 7,8]. We use the Tillotson [9] equation of state formulation. The simulations use 200,000 particles, with a mean particle diameter of 118 km.

Initial conditions. Planetary-scale impacts occurred predominantly at the end of accretion, and therefore the, in these studies a Mars-like planet, has properties matching those modeled for a young, post-accretional Mars [10,11,12]. The planet is set to have no pre-impact spin in the simulations.

Impact parameter space. We simulate impacts with energies of 0.13–5.89x10^{29} J (nominal 4,000 to 12,000 km diameter impact craters from gravity regime crater scaling laws into half-space targets; [13]), velocities of 6–50 km/s (about Mars' escape velocity to twice its orbital velocity), and impact angles of 0° (vertical, head-on impact) to 75°. The simulated maximum impactor to planet mass ratio is 0.09, ~50% smaller than the 0.12–0.25 impactor to Earth mass ratio for the Moon-forming event [14].

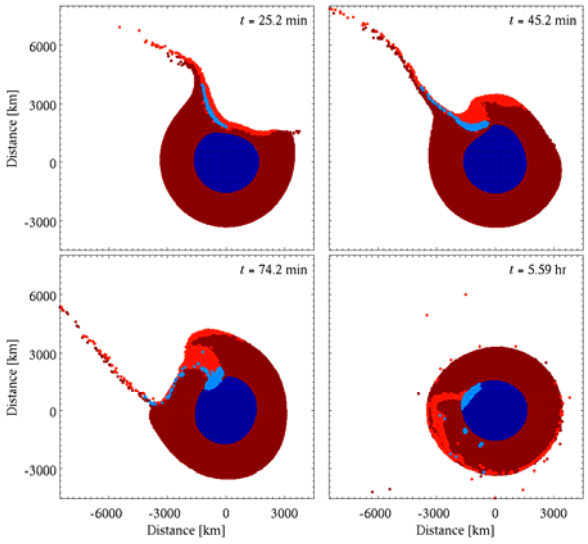

Figure 1. Oblique impact by a differentiated impactor. Simulation snapshots showing the sweeping of a differentiated impactor through the mantle of the planet; E_k = 3.14x10^{29} J, v_{imp} = 6 km/s, γ = 45°. Red and blue represent olivine and iron, respectively; darker shades are planetary material. Most of the impactor core accretes, while the rest is in the "ejecta tail."

As in [1] we use the pressure-dependent forsterite melting criterion [1,15] to calculate the total melt production, including melt at depth in the mantle.

Results: Our results provide information on the effects of impactor characteristics on the resulting impact process and geophysical signature. For the range of impact conditions, we investigate the impact process, the crater size and crustal redistribution, the melt production and distribution, the orbiting and ejected material, and the angular momentum transfer efficiency. Combining our new simulations with results for basalt impactors [1], we can discuss the variation in impact outcomes for a comprehensive range of impactor density and material composition (fig. 2). The simulated impactor types bracket the possible range of impactor compositions and internal structures expected for non-icy, planetary-scale impacts in the inner Solar System.

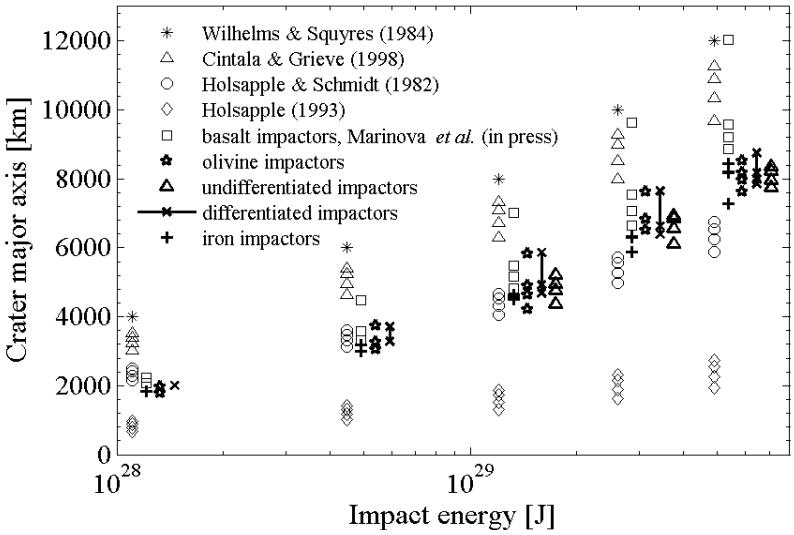

Figure 2. Crater sizes from our planetary-scale impact simulations and small, half-space impacts scaling relations, for head-on impacts. Simulation results for basalt (Marinova et al., submitted), olivine, undifferentiated, iron, and differentiated impactors are shown. For each impact energy, impact velocities of 6, 15, 25, and 50 km/s are plotted, if the conditions were simulated. Symbols are offset slight horizontally for

At a given impact energy and velocity, the impactor composition – and density – affect the size of the impactor. A smaller cross-sectional area of the impactor, while carrying the same total momentum and impact energy, alters the depth of penetration of the impactor, and thus where the majority of the energy of the impact is deposited. The location of deposition of the energy alters the resulting crater size, the location of the produced melt, the location of the antipode, and the crater shape. In addition, for oblique impacts, the large relative size of the impactor with respect to the target can result in only part of the impactor impacting the planet and thus affects the orbiting and escaping material, momentum transfer, and final rotational period (e.g., fig. 1). The results show that overall the impactor type affects the depth of penetration, the melt production, the surface melt cover, and the amount of orbiting and escaping material.

Over the simulated range, we find that the resulting crater cavity sizes are not sensitive to the impactor density or composition (fig. 2), however, the shape of the cavity is especially sensitive to the presence of a coherent iron component in the impactor. With increasing impactor density, the crater cavity is elliptical for a large range of impact conditions, consistent with the commonly elliptical planetary-scale impact basins that are observed on the planets (e.g., South Pole–Aitken basin on the Moon [16], Hellas Basin on Mars [17], Caloris Basin on Mercury [18]). As with the crater size, the antipodal cavity size is also not affected by the impactor composition. In examining the melt production, we find that the total melt amount produced is very sensitive to the impactor type, as is the partitioning of the melt between the mantle, surface, and ejecta reservoirs. Interestingly, the net effect is that the total melt production to surface melt cover relationship is similar for all impactor types. The impactor density is also important for the angular momentum transfer efficiency, where denser impactors impart a faster rotation rate on the target.

References: [1] Marinova M. M., et al. (in press) *Icarus*. [2] Lee D.-C. and Halliday A. N. (1996) *Science, 274*, 1876-1879. [3] Thomas P. C. et al. (2005) *Nature, 437*, 224-226. [4] McCord T. B. et al. (1970) *Science, 168*, 1445-1447. [5] Thomas P. C. et al. (1997) *Icarus, 128*, 88-94. [6] Benz W. (1990) NATO ASI series C. [7] Canup R. M. (2004) *Icarus, 168*, 433-456. [8] Asphaug E. et al. (2006) *Nature, 439*, 155-160. [9] Tillotson (1962) GA-3216, General Atomics. [10] Bertka C. M. and Fei Y. W. (1998) *EPSL, 157*, 79-88. [11] Sanloup C. et al., (1999) *Phys. Earth and Planet. Interiors, 112*, 43-54. [12] Hauck S. A. and Phillips R. J. (2002) *JGR-Planets, 107*, 5052-5071. [13] Wilhelms D. E. and Squyres S. W. (1984) *Nature, 309*, 138-140. [14] Canup R. M. (2008) *Icarus, 196*, 518-538. [15] Asimow P. D. (2007) Goldschmidt Conf. [16] Spudis P. D. et al. (1994) *Science, 266*, 1848-1851. [17] Andrews-Hanna J. C. et al. (2008) *Nature, 453*, 1212–1215. [18] Fassett, C. I. et al. (2009) *EPSL, 285,* 297–308.